A polar plot of the path of the spin axis for a simulated scan starting at an initial polar angle of 15° with a 6° increase per day is shown in Fig. 3. The equations used to simulate the scan were Eqs. (11) and (12), which include the orbital time variations (600-naut-mile orbit) in the magnetic field components. This scanning trajectory was obtained by starting the coil current at the proper initial phase angle, $(E - \sigma) = 76.6°$ (Fig. 2), and by supplying the required coil current in an open-loop fashion according to Eq. (18). The coil current required at any time during the scan was calculated from the time lapsed from scan commencement. That is, at any time t, $\lambda(t) = \gamma_o/2\pi\, t + \lambda(0)$, which gives the required magnetic moment m from Eq. (18) at time t after Eq. (17) has been used to find the nominal phase angle at time t. Thus, in practice, the control system can be mechanized with a clock to provide the time lapsed from the beginning of the scan along with the knowledge of the initial polar angle.

The simulated points in Fig. 3 are the location of the spin axis at $\frac{1}{20}$-day intervals after scan initiation. Hence, if the scan proceeded exactly on the desired nominal pattern, these points would appear at 18° precession angle intervals. The deviation from the nominal pattern is caused by the orbital variation in the magnetic field which was removed by averaging in determining the nominal control. Studies of the effects of error sources for the system, such as the magnetic field model, indicate that the polar angle behavior is more sensitive to error than the precession angle. For example, if the simulation for the conditions applying to Fig. 3 is repeated with an actual dipole tilt of 20° while the control current is based on 11°, the precession angle still increases very nearly at one revolution per day while the polar angle oscillates with an amplitude of $\sim$9° while increasing at 9° per day. As with all open-loop systems, the addition of feedback control may be required to overcome the orbital and other disturbances if close adherence to the nominal scan pattern is desired.

The torque caused by the gravitational field can also be counteracted by the control system. The gravity-gradient torque is given by $\tilde{T} = 3\omega_o^2\tilde{\xi} \times I \cdot \tilde{\xi}$ where $\tilde{\xi}$ is the outward geocentric unit vector at the satellite and I is the satellite moment of inertia dyadic. If the components of this torque are included in the state equations [Eqs. (1–5)] along with the magnetic control torques and the equations for the average motion are formulated, the equations, comparable to Eqs. (13) and (14), which result are

$$\dot{\lambda} = (-mB_o\, c\theta\, s\delta/2h)\, c(E - \sigma) \quad (19)$$

$$\dot{\sigma} = \frac{-mB_o\, c\theta}{2h\, s\lambda}\, [s\delta\, c\lambda\, s(E - \sigma) + 2\, c\delta\, s\lambda] + \frac{3\omega_o^2(I_3 - I)\, c\lambda}{4h}\, [1 - 3\, c^2\theta] \quad (20)$$

with h and θ constant. The only change resulting from the gravitational torque is the last term in Eq. (20), which represents the average effect per orbit of the gravitational torque on the spin axis precession rate $\dot{\sigma}$. In this term I_3 is the spin axis moment of inertia and I is the transverse moment of inertia. If the scan pattern described by $\lambda(t) = (\gamma_o/2\pi)\dot{\sigma}t + \lambda(0)$ with $\dot{\sigma} = \omega_E$ is again desired, and if the scan is initiated with $\theta = 0$, the phase angle requirement is

$$(E - \sigma) = \sin^{-1}[\gamma_o\, \mathrm{ctn}\delta/C\pi] - \alpha \quad (21)$$

where

$$C = [(1 + b)^2 + (\gamma_o\, \mathrm{ctn}\lambda/2\pi)^2]^{1/2}$$

$$\tan\alpha = -2\pi(1 + b)\tan\lambda/\gamma_o$$

and

$$b = 3\omega_o^2(I_3 - I)\, c\lambda/2h\omega_E$$

The magnetic moment required can be found from either Eq. (19) or Eq. (20) using the value of $(E - \sigma)$ from Eq. (21). Thus, the control system can also be designed to provide the scan while counteracting the averaged gravitational torque.

References

[1] Fleig, A. J., "A Passive Method for Scanning the Celestial Sphere," *Journal of Spacecraft and Rockets*, Vol. 6, No. 7, July 1969, pp. 846–847.

[2] Beletskii, V. V., "Motion of an Artificial Satellite About its Center of Mass," TT F-429, 1966, NASA, pp. 108–110.

[3] Wheeler, P. C., "Magnetic Attitude Control of Rigid Axially Symmetric Spinning Satellites in Circular Earth Orbits," SUDAER 224, April 1965, Stanford University, Palo Alto, Calif.

[4] Johnson, F. S., ed., *Satellite Environment Handbook*, Stanford University Press, Stanford, Calif., 1965, p. 165.

[5] Volosov, V. M., "The Method of Averaging," *Soviet Mathematics*, Vol. 2, No. 2, March 1961, pp. 221–224.

[6] Hedgepeth, J. and Schuerch, H., "Large Law Frequency Orbiting Radio Telescope," CR-1201, Oct. 1968, NASA.

Parameter Sensitivity of Aerodynamic Coefficients Determined from Experimental Data

Charles F. Huff,* Robert B. Asher,† and Henry R. Sebesta‡

Oklahoma State University, Stillwater, Okla.

Nomenclature

$C_{m\alpha}$ = restoring moment coefficient due to angle of attack, rad^{-1}
$C_{mp\beta}$ = magnus moment coefficient due to angle of attack and roll rate, rad^{-2}
C_{mq} = damping moment coefficient due to inertial angular rates, rad^{-1}
d = body diameter, ft
E = noise or error variation in the data, rad
I_x = roll moment of inertia about body x axis, slug-ft^2
I = lateral moment of inertia, slug-ft^2
$M_{p\beta}, M_q$ = magnus and damping moments, ft-lb-sec/rad^2
M_α = restoring moment, ft-lb/rad
p = roll angular velocity, rad/sec
q' = dynamic pressure, psf
S = body cross-sectional area, ft^2
t = time, sec
V = total free-stream velocity, fps
$\bar{\alpha}, \bar{\beta}$ = angles of attack and sideslip, rad
ζ = $pI_x/2I$, rad/sec
$\lambda_{1,2}$ = damping exponent, sec^{-1}
ξ = complex total angle of attack, rad; subscripts a and d indicate analytical solution and data, respectively
Φ = performance index
$\omega_{1,2}$ = nutation and precession frequencies, rad/sec

Introduction

AERODYNAMIC force and moment coefficients for missiles are commonly determined by performing wind-tunnel or free-flight tests and using analytical techniques to extract the coefficients. Unrealistic values may result because of lack of sensitivity of the analytical solution in the test range to changes in the coefficients and to data noise. Severe problems can arise in analyzing resonant motion, because the behavior is very sensitive to the coefficient values. This Note presents an analytical concept for predicting the effectiveness of data

Received June 2, 1970; revision received July 30, 1970.

* Graduate Student. Member AIAA.

† 2nd Lt. USAF; also Graduate Student. Member AIAA.

‡ Associate Professor. Member AIAA.

reduction analyses. A key part of the reduction analysis is specification of an index of the effectiveness of the data fit to the assumed solution, e.g., the integral of the square of the difference between the data and the assumed solution. The second-order sensitivity of this index to changes in the coefficient values indicates the potential for erroneous results. Minimization of the index assumes a best coefficient fit in the least-squares sense.

Sensitivity Analysis

The coefficients are to be determined so as to minimize

$$\Phi = \int_{t_1}^{t_2} (|\xi_d - \xi_a|)^2 dt \qquad (1)$$

where ξ_d is the experimental value and ξ_a is the solution of the analytical model for which coefficients are to be determined. The function used for Φ is arbitrary. It should be noted that $\xi_d = \xi_a + E$, where E is the noise that remains in the filtered data and/or variation due to model selection.

In order to identify when a problem may arise, a measure of sensitivity must be formulated. The partial derivatives

$$\partial\Phi/\partial C_{m\alpha} = 0, \quad \partial\Phi/\partial C_{mq} = 0, \quad \text{and } \partial\Phi/\partial C_{mp\beta} = 0 \qquad (2)$$

represent necessary conditions that may be solved for the coefficients, $C_{m\alpha}$, C_{mq}, and $C_{mp\beta}$, which minimize Φ in Eq. (1). These equations may be considered to be the sensitivity of the performance index to the respective aerodynamic coefficients.

Equation (1) may be expressed as a differential equation by differentiating both sides to yield

$$\dot{\Phi} = (|\xi_d - \xi_a|)^2, \quad \Phi = 0 \text{ at } t = t_1 \qquad (3)$$

The first-order sensitivity coefficients satisfy

$$\frac{d}{dt}\left(\frac{\partial\Phi}{\partial C_i}\right) = (\xi_a - \xi_d)\frac{\partial\bar{\xi}_a}{\partial C_i} + (\bar{\xi}_a - \bar{\xi}_d)\frac{\partial\xi_a}{\partial C_i}, \quad \frac{\partial\Phi}{\partial C_i} = 0 \qquad (4)$$

at $t = t_1$; $i = m\alpha, mq, mp\beta$.

The set of second-order sensitivity coefficients may be obtained by differentiating Eq. (4) with respect to the elements C_j.

$$\frac{d}{dt}\left(\frac{\partial^2\Phi}{\partial C_i C_j}\right) = (\xi_a - \xi_d)\frac{\partial^2\bar{\xi}_a}{\partial C_i C_j} + \left(\frac{\partial\xi_a}{\partial C_i}\right)\left(\frac{\partial\bar{\xi}_a}{\partial C_j}\right) + (\bar{\xi}_a - \bar{\xi}_d)\frac{\partial^2\xi_a}{\partial C_i C_j} + \left(\frac{\partial\bar{\xi}_a}{\partial C_i}\right)\left(\frac{\partial\xi_a}{\partial C_j}\right) \qquad (5)$$

$\partial^2\Phi/\partial C_i\partial C_j = 0$ at $t = t_1$; $i = m\alpha, mq, mp\beta$; $j = m\alpha, mq, mp\beta$

The second-order sensitivity coefficients will give information as to how sensitive the first-order necessary conditions are to changes in the optimal parameters. If ξ_a or Φ is relatively insensitive to a change in a coefficient, then optimum parameter determination may be inaccurate. Additional details on the development and application of second-order sensitivity coefficients are available in Ref. 3.

Figure 1 illustrates the dependence of Φ on the coefficients for a typical example. The partial derivatives ("sensitivity coefficients") may be approximated from the plots. The lines of constant Φ (i.e., Φ_c) are given by Φ = const in Eq. (1) where ξ_a is the analytical solution with coefficient values on Φ_c lines. The Φ_c lines indicate possible range of coefficient values for $\Phi_{\min} = \Phi_c$. It is apparent that Φ is quite sensitive to changes in $C_{m\alpha}$, but relatively insensitive to changes in C_{mq} or $C_{mp\beta}$. The sensitivity of Φ with respect to the two damping terms is about equal as shown in Fig. 1. Thus, accurate determination of C_{mq} or $C_{mp\beta}$ from experimental data is quite difficult. The sensitivity coefficients are only slightly affected by E near $\Phi_{\min}$. The E generally increases $\Phi_{\min}$ and shifts its location away from the true coefficient values.

Examples

A particular analytical model is chosen to illustrate the problem; however, the concepts are independent of the model. For instance, a particular model for the angular motion of a missile can be described by a linearized approximate form of the equations of motion for angle of attack given by[1]

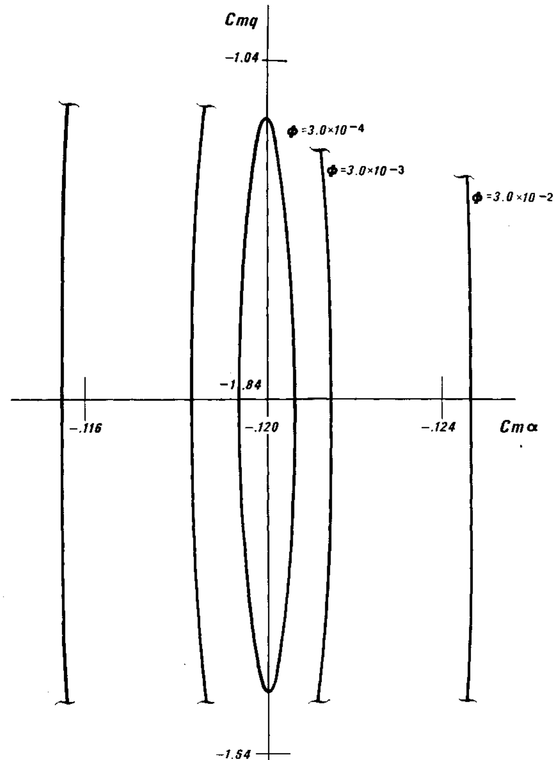

Fig. 1a Contours of constant Φ_c for $C_{mp}\beta$ = 0.0 for reentry vehicle, example.

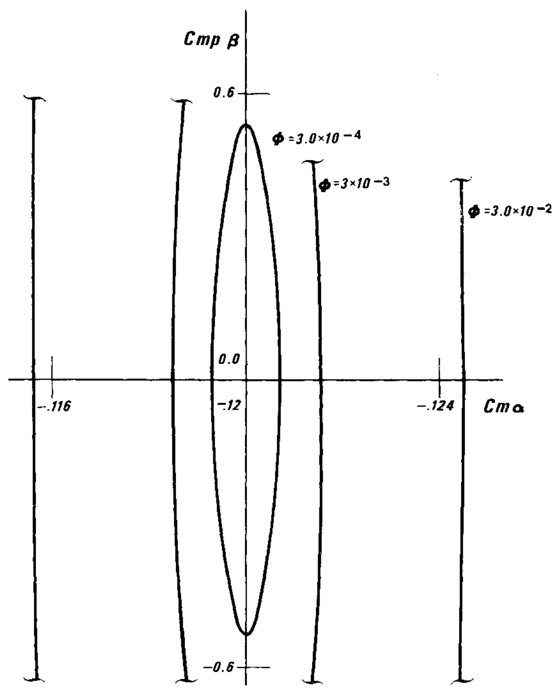

Fig. 1b Contours of constant Φ_c for C_{mq} = −1.84 for reentry vehicle, example.

$$\ddot{\xi} + [-ip\, I_x/I - (M_q + M_{\dot{\alpha}})/I]\dot{\xi} + (-ip\, M_{p\beta}/I - M_\alpha/I)\xi = 0 \qquad (6)$$

where $M_\alpha = C_{m\alpha}q'Sd$; $M_q + M_{\dot{\alpha}} = C_{mq}q'Sd^2/2V$; and $M_{p\beta} = C_{mp\beta}q'Sd^2/2V$. This equation has a solution of the form $\xi = i\bar{\alpha} + \bar{\beta}$ where

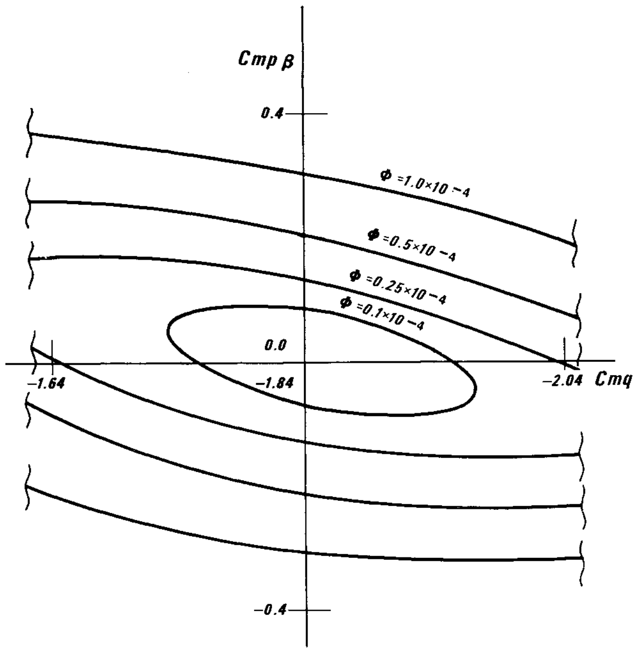

Fig. 1c Contours of constant Φ_c for $C_{m}\alpha = -0.12$ for re-entry vehicle, example.

$$\bar{\alpha} = (A_1 \cos\omega_1 t + B_1 \sin\omega_1 t)e^{\lambda_1 t} + (A_2 \cos\omega_2 t + B_2 \sin\omega_2 t)e^{\lambda_2 t}$$

$$\bar{\beta} = (B_1 \cos\omega_1 t - A_1 \sin\omega_1 t)e^{\lambda_1 t} + (B_2 \cos\omega_2 t - A_2 \sin\omega_2 t)e^{\lambda_2 t}$$

and with $\zeta \equiv pI_x/2I$,

$$\lambda_{1,2} = \left(\frac{M_q + M_{\dot{\alpha}}}{2I}\right)\left[1 \pm \frac{\zeta}{(\zeta^2 - M_\alpha/I)^{1/2}}\right] \pm \frac{\zeta M_{p\beta}/I_x}{(\zeta^2 - M_\alpha/I)^{1/2}}$$

and $\omega_{1,2} = \zeta \pm (\zeta^2 - M_\alpha/I)^{1/2}$.

The coefficients to be determined are $C_{m\alpha}$, C_{mq}, and $C_{mp\beta}$ where $C_{m\dot{\alpha}}$ is incorporated into C_{mq}.

As a particular example a small reentry vehicle entering the Earth's atmosphere is presented with the q' curve from Ref. 2. The aerodynamic coefficients of the vehicle are $C_{m\alpha} = -0.12$, $C_{mq} = -1.84$, $C_{mp\beta} = 0$. The time interval was 2.5 sec, which represents $\sim$3 cycles of motion. The initial value of α was 2° and p was 18.8 rad/sec. A case was run with $C_{m\alpha}$ and C_{mq} assumed known and $C_{mp\beta}$ to be determined. The sensitivities of Φ to coefficient variations for this model can be seen in Fig. 1. Simulated random noise was added to the actual solution (shown in Fig. 2), and the coefficient that gave a minimum Φ was determined. The effect of the noise is to increase $\Phi_{\min}$ from 0 to 0.0016 and $C_{mp\beta}$ from 0 to 0.6. The significance of such a difference in coefficient value must be judged in terms of the subsequent application of the results in other regions where the solution is sensitive to the coefficient value (e.g., resonant motion).

Another example is taken directly from Ref. 1. The vehicle is a finned rocket with $C_{mq} = -1400$ and $C_{mp\beta} = 0$. The data was generated directly from Eq. (1) using an α dependent $C_{m\alpha} = -31 + \epsilon$, where $\epsilon = 0.01(10 - |\xi|)^2$ over an interval of $\sim$8 cycles with $\xi = 10°$ at t_1. The minimum Φ of 0.448 was achieved with the computed parameters $C_{m\alpha} = -29.8$ and $C_{mp\beta} = -40$, where C_{mq} was held constant at -1400. The average amplitude error was only 0.238°, or 2.4%. It should be noted that with a Φ of this size for this example the values calculated for $C_{m\alpha}$ and $C_{mp\beta}$ could be further from the actual values depending on the error form. The sensitivity of Φ to coefficient variation is similar to the previous examples. The data used in the examples have much less distortion than typical experimental data.

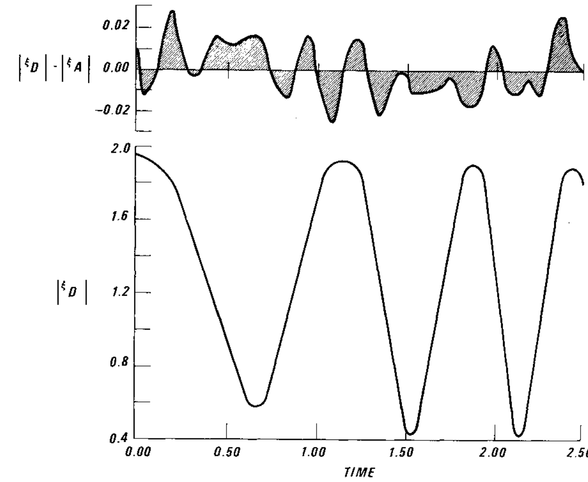

Fig. 2 Plot of data in degrees and error in degrees vs time.

Conclusions

Use of a sensitivity analysis of a performance index Φ has shown that it may be difficult to determine aerodynamic coefficients accurately from experimental data because of the insensitivity of the solution to variations in these parameters. In addition, techniques which obtain coefficient values should be carefully evaluated to make certain that they do not use one insensitive parameter in the determination of another parameter. A perfect fit ($\Phi = 0$) can never be achieved because of variation in the data from the assumed solution. These variations or errors come from data noise, modeling errors, and time-varying parameters. Experimental data should be obtained in regions of maximum coefficient sensitivity.

References

[1] Vaughn, H. R., "A Detailed Development of the Tricyclic Theory," SC-M-67-2933, Feb. 1968, Sandia Labs., Albuquerque, N. Mex.

[2] Vaughn, H. R., "Spin-up and Roll Reversal of Reentry Vehicles," SCRR 68-219, May 1968, Sandia Laboratories, Albuquerque, N. Mex.

[3] Unruh, D. R., "Determination of Optimal Parameters for Dynamical Systems," Ph.D. dissertation, 1970, Oklahoma State University, Stillwater, Okla.

Aerodynamic Viscous Effects on a New Space Shuttle Vehicle

M. I. Kussoy,* C. C. Horstman,† and D. A. Stewart‡
NASA Ames Research Center, Moffett Field, Calif.

Introduction

A NEW configuration for a reusable space shuttle vehicle (SSV) was presented and discussed by Faget.[1] Plan views of this vehicle, taken from Ref. 1, are shown in Fig. 1. The short-range shuttle will spend between 150 and 200 sec of flight time descending from the entry altitude of 400 K to 300 K ft at a Mach number around 25. Previous results for blunt lifting reentry bodies,[2] such as the Apollo, have indicated significant viscous effects on the forces over these

Received July 8, 1970.
* Research Scientist. Member AIAA.
† Research Scientist. Associate Fellow AIAA.
‡ Research Scientist.